SLAC–PUB–6385
October 1993
(A)

# MUON BACKGROUND IN A 1.0-TEV LINEAR COLLIDER*

L. P. Keller

*Stanford Linear Accelerator Center*
*Stanford University, Stanford, California 94309*

## 1. INTRODUCTION

The first detailed, quantitative study of muon background in a linear collider was done by G. Feldman in 1988 for the Mark II detector at the Stanford Linear Collider (SLC). This followed the observation of an intolerable number of muons coming from beam-halo collimators in the SLC final focus. For his study of the problem, Feldman wrote the program MUCARLO, Version 1.0, which successfully reproduced the experimental results for the number and spatial distribution of muons hitting Mark II. The background in Mark II, and subsequently SLD, was reduced to a tolerable level by installing magnetized iron spoilers in the final focus tunnels and by adding beam scrapers in the last three sectors of the linac, approximately 1500 meters from the collider hall and separated from the detector by the SLC arcs. For application to a true linear collider, MUCARLO was modified to include variable-energy primary beams up to 250 GeV and a linac with optical lattice and waveguide in front of the final focus. The results[1] of that study were that for a 250 GeV electron beam impinging on a source at the entrance to the final focus (497 m from the interaction point (IP)), the loss of $3.7 \times 10^7$ beam particles resulted in one muon in a 6.1 m square defined as the detector. This was about a factor of 150 improvement over the same conditions without magnitized iron spoilers in the final focus.

* Work supported by Department of Energy contract DE–AC03–76SF00515.

More recently the Next Linear Collider (NLC) design group at SLAC has included a collimation system between the linac and final focus which will continuously intercept up to 1% of a 500 GeV beam, or an average power of 84 kW.[2] The collimation system consists of a sequence of six spoiler/total absorber combinations. It is separated from the final focus by a 10-mrad "big bend" which generates a crossing angle at the IP, allows switching between multiple IPs, and aids muon protection. The main sources of muons for the study described here are the six Hi-Z total absorbers in the collimation system. This study expands on the work in Ref. 1 by including: a 500 GeV beam (instead of 250 GeV); direct $e^+$ annihilation, $e^+e^- \rightarrow \mu^+\mu^-$ (in addition to Bethe-Heitler pair production, $\gamma Z \rightarrow Z\mu^+\mu^-$); and a calculation of muons from photopion production, $\gamma A \rightarrow X\pi(\pi \rightarrow \mu\nu)$.

The NLC group's design parameters for a 1 TeV center-of-mass linear collider are $1.3 \times 10^{10}$ particles/bunch, 1.4 nsec bunch spacing, 67 bunches/train, and 120 bunch trains/sec.[3] This is $8.7 \times 10^{11}$ beam particles in a 96 nsec bunch train. The design goal of this study was to construct a system of spoilers which will limit the muon background to less than one muon in a 4.5-m-radius detector for 1% of a bunch train (approximately $10^{10}$ beam particles) lost in the collimation section. This goal is based on the possibly conservative assumption that the time resolution of the detector would not be able to correlate a muon from anywhere in the pulse train with a particular bunch crossing.

## 2. DESCRIPTION OF THE MONTE CARLO PROGRAM

For completeness, some of the features of MUCARLO which were described in Ref. 1 will be repeated here, and new features and changes will be noted.

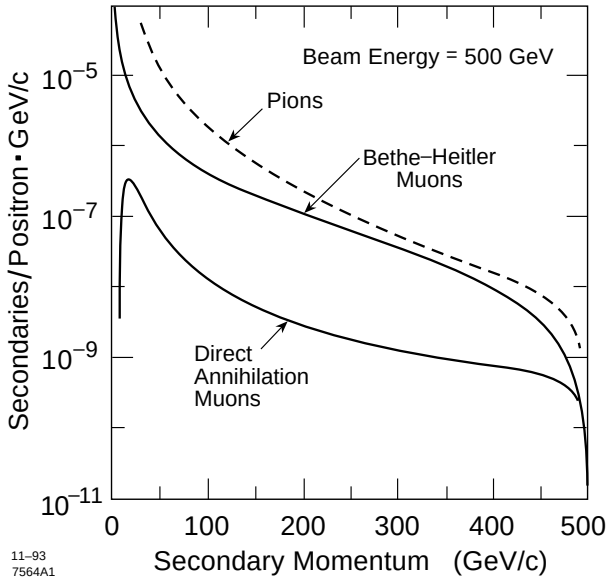

Figure 1. Secondary muon and pion yields from 500 GeV electrons and positrons incident on a 20 rl tungsten target.

## 2.1 Production

Figure 1 shows the secondary muon and pion yields in 1 GeV/c bins versus secondary momentum for 500 GeV incident electrons and positrons on a 20 rl tungsten target. The production mechanisms are explained below.

*A. Bethe-Heitler*

The expression for the differential cross section $d\sigma/dp_\mu d\theta_\mu$ for the Bethe-Heitler process ($\gamma Z \rightarrow Z\mu^+\mu^-$) is given by Y. Tsai.[4] For a given photon energy $k$ the differential cross section is evaluated for a large number of momentum-angle bins. The total number of events in each momentum-angle bin is then given by the product of the differential cross section and the photon path length $d\ell(k)/dk$ summed over all possible photon energies. The photon path length is calculated using the Clement-Kessler shower approximation,

$$\frac{d\ell(k)}{dk} = \frac{.964 X_o/E_{\rm beam}}{-\ell n(1-\mu^2) + .686\mu^2 - 0.5\mu^4} \quad ,$$

where $\mu = k/E_{\rm beam}$, and $X_o$ is the radiation length of the source material. In Fig. 1 the curve labelled "Bethe-Heitler Muons" is the result of this calculation. It applies to both electron and positron beams incident on the source.

*B. Direct $e^+$ Annihilation*

The laboratory threshold energy for the annihilation of positrons on atomic electrons is 43.7 GeV. In the center-of-mass the differential cross section for $e^+e^- \to \mu^+\mu^-$ is

$$\frac{d\sigma}{d\Omega} = \frac{\alpha^2}{8E_{e^+}^2}(1+\cos^2\theta) \quad ,$$

where $\alpha^2 = 20.8nb \cdot \mathrm{GeV}^2$ and $E_{e^+}$ ranges from 0.1056 GeV at threshold to 0.357 GeV at 500 GeV in the laboratory.

The differential cross section is evaluated in $\theta_\mu$ bins and transformed to the laboratory in the same $p_\mu, \theta_\mu$ bins used in the Bethe-Heitler distribution. The total number of events in each momentum-angle bin is then given by the product of the differential cross section and the $e^+$ path length determined from the EGS4 shower program and summed over all $e^+$ energies from threshold to beam energy. Since the $e^+$ shower spectrum is much softer for a primary electron beam than for a primary positron beam, this production mechanism is only included for the $e^+$ side of the linear collider. In Fig. 1 the curve labelled "Direct Annihilation Muons" is applicable only to the positron side of the linear collider. Note that this process is comparable to Bethe-Heitler near the end-point of the muon production spectrum.

*C. Photopion Production*

Pion production from a tungsten target is calculated using the program EGS-FLUKA.[5] The muon spectrum from pion decay ranges from approximately half the pion momentum to nearly the full pion momentum. However, the decay length for a 500 GeV pion is 27.8 km, so that only a small fraction of pions will decay before they interact in material downstream from the source. It is seen

from Fig. 1 that even if 10% of all pions produced turn into muons of the same momentum, this mechanism is still small compared to Bethe-Heitler.

*D. Sources*

The source can be placed anywhere between the entrance to the linac and the IP. The source material and thickness are variables, and unless otherwise specified, the results presented here are for 20 rl of tungsten. Using the input beam energy, the program randomly selects the muon momentum and angle from the source distribution. For source locations in the linac, where the beam has not reached final energy, the momentum-angle distribution is based upon the beam energy at that point.

Before exiting the source, the muon undergoes multiple coulomb scattering and energy loss. Most of the muons are produced within a few units of the critical angle $\theta_c = m_\mu/E_\mu$; so that for a given muon momentum and a 20 rl source, the ratio of production angle to scattering angle is $\theta_c/\theta_{\rm MCS} \approx 1.6$.

**2.2 Beam Line and Linac**

Figure 2 shows a schematic of the collimation and final focus beam transport sections used in this study.[6] Note the different scales in the transverse and longitudinal directions. The collimation section has a series of six Hi-Z collimators and a total bend of 6.14 mrad followed by a "big bend" with a total bend of 10 mrad followed by the final focus with a reverse bend chromatic correction section of $\pm 2.21$ mrad bends. The model includes a 3.05-m-square cross section concrete tunnel through sandstone, concrete support girders under the beam elements, and dipoles and quadrupoles which include return flux in the iron and pole tips. The detector is assumed to have a 4.5-m-radius cross section centered on the IP. There is a series of magnetized iron spoilers of alternating polarity distributed through the final focus. Figure 3 shows how the spoilers are arranged in the tunnel at a given location. The field in the iron was modelled using the two-dimensional program POISSON.[7] Each spoiler is 9.1 m long with a winding slot width and height of

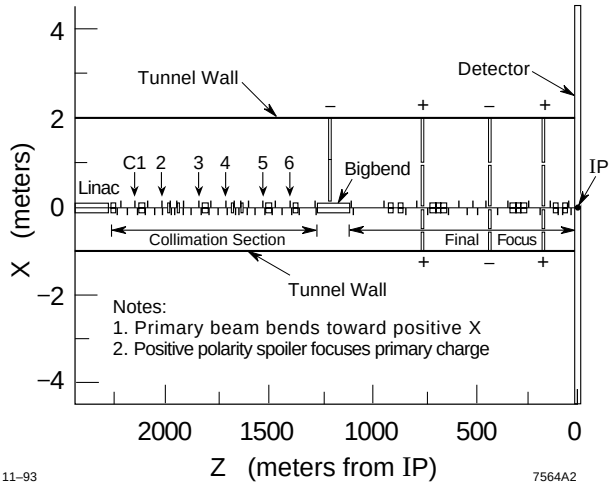


Figure 2. Plan view of the NLC beam line in the tunnel with magnetized iron spoilers.

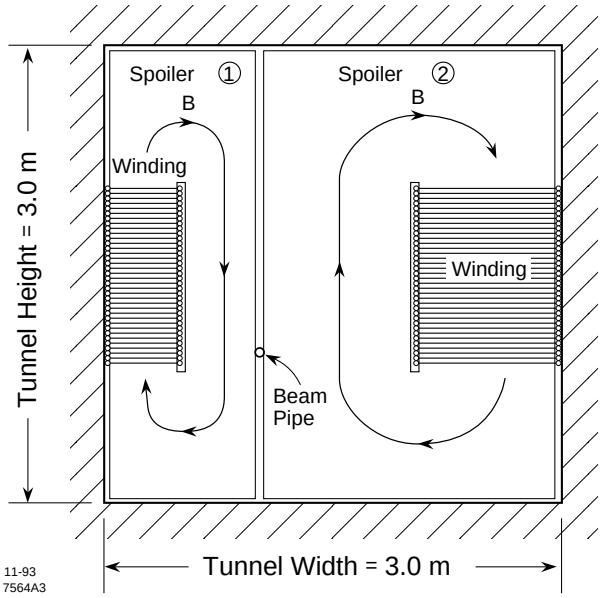


Figure 3. Two side-by-side magnetized iron spoilers filling a $3\times3$ meter beam tunnel.

3.2 cm and 126 cm, respectively. Each set of "tunnel-filler" spoilers weighs 750 tons and would cost \$2–3 million installed. For magnitized iron with a field of 16 kG, the ratio of bend angle to scattering angle is $\theta_{\rm bend}/\theta_{\rm MCS} \approx 3\sqrt{L}$, where $L$ is the length of the spoiler in meters.

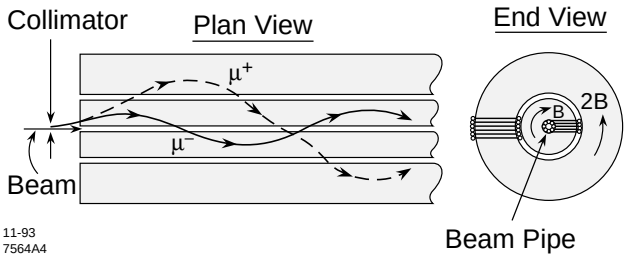

Figure 4. Nested, magnetized iron cylinders of opposite polarity to channel both $\mu^+$ and $\mu^-$.

An alternative to large tunnel-filler magnitized iron spoilers has been proposed.[8] It consists of nested iron cylinders with opposite-polarity azimuthal magnetic fields as shown in Fig. 4. The idea is that the nested cylinders are located downstream from each muon source and are long enough to either range out muons or cause enough energy loss so that the muon is unlikely to reach the detector. A version of the nested cylinder idea was tried in MUCARLO, and the results are presented in Section 3.

The linac lattice is a FODO design[9] in which the quadrupole strengths and spacing scale as $E^{1/2}$ between the beginning and end of the linac. The linac model includes the 11.4 GHz waveguide, support girder, FODO lattice quadrupoles, and the same tunnel size as for the collimation and final focus sections.

### 2.3 Muon Tracking

After the muon exits the source, the Monte Carlo program swims it in 30 cm steps thru the tunnel. When material is encountered, the muon scatters, loses energy, and bends (if magnetic field is present). The trajectory of each muon is followed until the muon either stops or reaches the IP. For the purposes of this study, the details of the detector, e.g. trackers, calorimetors, and muon walls, are not included. A muon which reaches the IP within a radius of 4.5 m from the beam line is counted as a detector hit. A large variety of one- and two-dimensional histograms of the muon coordinates, direction, and momentum at any longitudinal

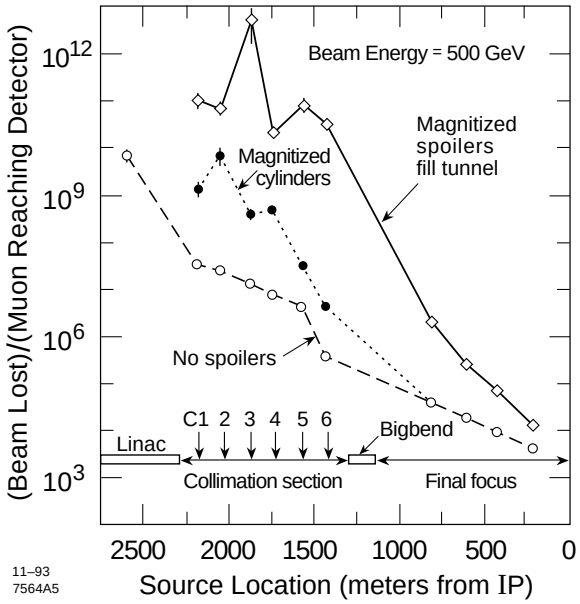


Figure 5. Results of muon Monte Carlo calculations for three conditions: no spoilers and two types of magnetized iron spoilers.

point in the tunnel can be generated. A particularly useful feature is an output file, in the TOPDRAW format, of individual trajectories of muons that reach the IP.

## 3. RESULTS

Figure 5 shows the number of beam particles which must hit a collimator to produce one muon in the detector as a function of source location in the beam line. As a worst case, an $e^+$ beam was chosen for this study so that direct annihilation production could be included. The source points include the six Hi-Z collimators in the collimation section and collimators at four high-beta points in the final focus, which are potential scrapers of beam-gas coulomb scattering or beam-gas bremsstrahlung.

From the curve labelled "No spoilers" it is seen that a beam loss of $10^{10}$/bunch train anywhere in the collimation section will result in a muon background which is many orders of magnitude away from the design goal. The curve labelled "Magnetized spoilers fill tunnel" in Fig. 5 is the result of adding magnitized iron

spoilers which fill the tunnel at three locations in the final focus and one magnetized iron piece in the tunnel aisle next to the 10 mrad big bend (See Fig. 2). It is seen that for all six collimators in the collimation section, more than $10^{10}$ beam particles must be lost to produce one muon in the detector. This satisfies the design goal of allowing a 1% continuous beam loss in the collimation section.

The curve labelled "Magnetized cylinders" in Fig. 5 shows the results of filling all drift spaces in the collimation section with magnetized iron cylinders as described in Section 2. The result is considerably worse than for magnetized iron spoilers which fill the tunnel and does not meet the design goal. This is because the magnetized cylinders must be interrupted by beam elements, especially dipoles in the chromatic correction sections, which disperse muons away from the cylinders and therefore disrupt the channeling orbits.

For the case of the magnetized iron tunnel-fillers, Fig. 6 shows histograms of muon-production momenta and final momenta for muons which hit the detector from the six sources in the collimation section. It is seen that the initial muon momentum must be greater than 300 GeV/c to hit the detector from sources outboard of the big bend. Figure 7 shows the spatial distribution of muons from the collimation section which reach the IP. It is seen that increasing the detector dimensions by 2–3 m in the horizontal direction would intercept significantly more muons.

## 4. SUMMARY AND CONCLUSIONS

For sources in the collimation section of a 1 Tev center-of-mass linear collider, a system of magnetized iron spoilers which fills the tunnel and meets the design goal of allowing a continuous 1% beam loss, or $10^{10}$ beam particles/bunch train, was found. This is more than a three orders of magnitude improvement over the case with no muon spoilers. For the case of magnetized iron cylinders which fill all drift spaces in the collimation section, the design goal was not met.

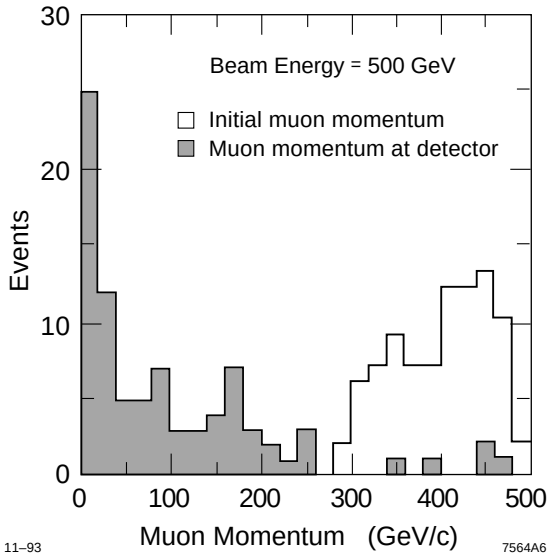


Figure 6. Momentum histograms for muons which hit the detector from six sources in the collimation section.

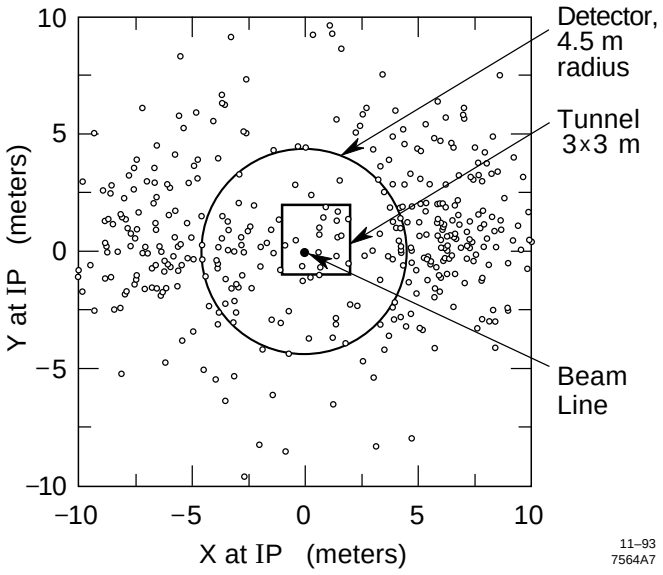


Figure 7. Spatial distribution of muons which reach the IP from six sources in the collimation section.

# REFERENCES


1. L. Keller, *Calculation of Muon Background in a 0.5 TeV Linear Collider*, SLAC–Pub–5533, April 1991.

2. J. Irwin, *et al., Conventional Collimation and Linac Protection*, SLAC–Pub–6198, April 1993.

3. J. Irwin, *Fifth International Workshop on Next-Generation Linear Colliders*, SLAC, October 13–21, 1993.

4. Y. Tsai, *Rev. Mod. Phys.,* Vol 46, No. 4, (1974), p. 815.

5. J. Ranft, *et al., The Hadron Cascade Code, FLUKA82: Setup and Coupling with EGS4 at SLAC*, SLAC–TN–86–3, April 1986.

6. R. Helm, TRANSPORT deck TLCFF5, June 1992.

7. R. Early, Private Communication.

8. E. Kushnirenko, *Proceedings of the International Workshop, on Final Focus and Interaction Regions of Next Generation Linear Colliders*, SLAC–405, March 1992.

9. K. Bane, Private Communication.